Iranian Journal of Medical Physics
ijmp.mums.ac.ir
IJMP

Evaluating the Performance of Various Detectors in the Small Field Size by 6 MV Linac

Saed J. Al Atawneh[1,2*]

1. Department of Radiation Oncology, King Hussein Cancer Center, Queen Rania St 202, Amman, Jordan
2. Department of Physics, Faculty of Science, Al-Balqa Applied University, P.O.Box: Al-Salt 19117, Jordan

ARTICLE INFO

Article type:
Technical Notes

Article history:
Received: Feb 14, 2022
Accepted: Apr 29, 2022

Keywords:
Detectors
Gafchromic Film
Film Dosimetry
Radiation Dosimetries

ABSTRACT

Introduction: We present a comprehensive evaluation of three different dosimeters in 6 MV flattening filter-free beam (FFF) under charged particle dis-equilibrium conditions.

Material and Methods: Diamond detector, Gafchromic film, and Un-shielded diode detector were used in this study. The total scatters factor of Jaw-shaped fields was measured starting from (10x10 cm^2) down to (0.5x0.5 cm^2) using True Beam Linear Accelerator (Varian) and solid water phantom.

Results: The diamond detector presented more accurate results at an ultra-small field size (0.5x0.5 cm^2) with a 14.1% deviation of the diode results. On the other hand, all the measurements ranged within 5% for large field sizes "i.e. Larger than 4.0x4.0 cm^2". The relative output factor (ROF) was introduced as a total scatter factor measured by a given dosimeter (x) to total scatter factor measured by diamond detector ($OF_x/OF_{diamond}$), the relative output factor values were 0.859 and 0.104 for both Diode/Diamond ($ROF_{Diamond}^{diode}$) and Film/Diamond($ROF_{Diamond}^{film}$), combinations, respectively.

Conclusion: We found that the diamond detector is the most appropriate detector for the small field dosimetry with high accuracy.

► *Please cite this article as:*
Al Atawneh S. Evaluating the Performance of Various Detectors in the Small Field Size by 6 MV Linac. Iran J Med Phys 2023; 20: 1-6. 10.22038/IJMP.2022.63725.2088.

Introduction

Recently, radiation therapy requirements play an important role in the development of therapeutic devices and treatment strategies. High-energy photon linacs can be distinguished into three subtypes: spiral linacs, robotic linacs, and normal linacs. While the conventional linac, which normally includes a flattening filter (FF) to produce a consistent dose at specific depths, might be used without one, the first two are not [1].

Different techniques used the flattening filter free (FFF) photon beams for radiotherapy treatment, especially for Stereotactic Radiation Surgery (SRS), Stereotactic Body Radiation Therapy (SBRT), Intensity Modulated Radiation Therapy (IMRT), and Volumetric Modulated Arc Therapy (VMAT) [1-5]. The major advantages of FFF generation are increased dose rate and reduced head scatter, which allows for shorter delivery times with reduced dose in the field. For IMRT and VMAT techniques, they are based on providing a non-uniform fluence distribution. Therefore, flattened beams are not required [1, 5-7]. Generally, these advanced techniques are used for delivery of small fields or segments under non-equilibrium conditions. A simple definition for small fields is still unknown. Since the field dimensions are usually smaller than the lateral range of the charged particles [1, 5, 8, 9]. In other words, compared to the field size, the lateral range of the electrons, rather than the forward range, is the critical parameter to the Charged Particle Equilibrium (CPE). Dosimetry of small beams suffers from the lack of lateral charged particle equilibrium (CPE) [5, 8, 10-12]. As such, they are easily affected by a) the size of the collimator aperture (*r*), b) the detector size (Volume), c) the beam energy, and d) the characteristic of tissue (Homogeneous or Heterogeneous tissue). For small field sizes, the total scatters factor value will be underestimated. Hence the dose will be overestimated "i.e. overdose".

Das et al defined the small field dosimetry, the problem of charged particle dis-equilibrium, and the total scatters factor corrections [8]. IAEA-AAPM Technical Reports Series (TRS) no.483 provided extensive data for the small field dosimetry using different kinds of ion chambers and detectors [5]. Charles et al. quantified the impact that a 1 mm error in the field size of the detector position had on total scatter factors and established tolerable uncertainties on total scatter factor at 1% in order to define the small field size. In order to study the precise effects of lateral electronic disequilibrium, photon scattering in the phantom, and source occlusion, the total scatters

**Corresponding Author:* Tel: 0036306224164; Email: saed.al-atawneh|@atomki.hu

factor was divided into additional factors for a theoretical definition of very small field size [9]. Masangetal et al., using different detectors under charged particle non-equilibrium conditions, provided a complete description of the total small-field scattering coefficient in the 6 MV and 10 MV flattening-filter-free photon beams and reached the same conclusion; The smaller the detector, the better (more accurate) the reading of the total scattering coefficient [1]. Lechner et al [13] discussed the difference in detector response when irradiated with FF beams and with FFF beams. Recently, Dwivedi et al [14] showed small-field dosimetry of a 6 MV photon beam without a flattening filter (FFF) using various detectors. The output factor, depth dose, and beam profile of small fields with dimensions ranging from 0.6x0.6 cm^2 to 6.0x6.0 cm^2 were measured using the 6 MV FFF photon beam. The five detectors, SNC125c, PinPoint, EDGE, EBT3, and TLD-100, were utilized. None of the previous studies described the total scatter factor measurements using Gafchromic Film/Diamond combinations under charged particles dis-equilibrium conditions for FFF-beam. Along this side, in this paper, we present a comprehensive evaluation of the performance of various dosimeters such as Gafchromic (EBT3) film, diode detector, and diamond detector in the small field size by 6 MV FFF-beam of the ordinary linac. In this work, the total scatters factor readings for the small field size (< 1.5 cm^2) of the diode/diamond detectors combination show a small deviation, emphasizing that the smaller the detector the better (more accurate) the total scatter factor readings are. On the other hand, the Gafchromic film method shows less precise for the FFF-beam measurement, especially for the ultra-small field (0.5x0.5 cm^2). Meanwhile, the deviation for the large field sizes (> 4 cm^2) among three different measurement detectors was within an acceptable range.

Materials and Methods

Materials

Linear accelerator and detectors

A True Beam Linear Accelerator (Varian) with 6 MV FFF/FFB capability, designed to deliver intensity-modulated radiation therapy, combined with solid water phantom (30x30x20 cm^3) was used for dose calibration and the total scatter factor measurements. All measurements were accomplished by three extraordinary detectors, see table 1.

Table 1. Characteristics of detectors used in this study.

Detectors	Detector Type	Sensitive Volume (mm)	Volume
PTW 30010 wellhofer Farmer	gas filled	radius 3.05 (mm) length 23 (mm)	0.65 (cm^3)
PTW 60023 Diode	Un-shielded diode	radius 0.75 (mm) length 0.018 (mm)	0.03 (mm^3)
PTW 60019 Diamond	Diamond	radius 1.10 (mm) length 0.001(mm)	0.004 (mm^3)

Gafchromic film

In the present paper, seven pieces of Gafchromic films with (2x7 cm^2) and one piece with (10x10 cm^2) for film calibration were prepared and eight pieces of Gafchromic films starting from (10x10 cm^2) down to (0.5x0.5 cm^2) for total scatter factor measurement. For films analysis, the Automatic Film Scanner (AFS) and image analysis software program (ImageJ) was used, Table 2 shows the Gafchromic film specifications.

Solid water phantom

The solid water phantom is a tool developed for photon and electron beam calibration. No need to pull, set up or fill water tanks and can calibrate to within 1% of actual dosage. Furthermore, solid water has no charge build-up problem and scatters and attenuates X-rays in the radiation therapy field in the same way as water. In this study, it was employed for photon beam calibrations, dose measurements, and absolute calibrations with no requirement for correction and scaling factors. Table 3 shows solid water phantom specifications.

Table 2. Characteristic of Gafchromic film used in this study

Property	Property GAFChromic™ EBT3 Film
Configuration	Active layer (28 μm) sandwiched between 125 μm matte-surface polyester substrates
Size	8” x 10”, other sizes available upon request
Dynamic Dose Range	0.1 to 20 G
Energy dependency	<5% difference in net optical density when exposed at 100 keV and 18 MeV
Dose fractionation response	<5% difference in net optical density for a single 25 Gy dose and five cumulative 5 Gy doses at 30 min. intervals
Dose rate response	<5% difference in net optical density for 10 Gy exposures at rates of 3.4 Gy/min. and 0.034 Gy/min
Stability in light	<5x10-3 change in optical density per 1000 lux-day
Stability in dark (pre-exposure stability)	<5x10-4 optical density change/day at 23 °C and <2x10-4 density change/day refrigerated

Table 3. Characteristics of solid water phantom used in this study

Depth Ionization Relative-to-water	Electron Density Ratio
Photon: 1.000 +/- 0.005	Solid Water HE / Water: 1.000 +/- 0.005
Electron: 1.000 +/- 0.005	
Mass density (g/cm^3): 1.032 +/- 0.005	
Electron Density (e-/cm^3 NA): 0.557 +/- 0.001	

Methods

Dose calibration, Dosimeter calibration

In the case of detector calibration, the solid water phantom was placed on the table top of linac such that the distance from the source to the surface (SSD) was100 cm, and the detector was set up within the phantoms such that its axis should always be perpendicular to the central beam axis (CAX), see figure 1. The center of the detector was located at the depth of maximum dose (d_{max}) and the absolute dose measurement at d_{max} was accomplished via calibrated ion chamber (Farmer ion chamber) first and then by a diamond detector [5]. Figure 1 shows the detector calibration setup.

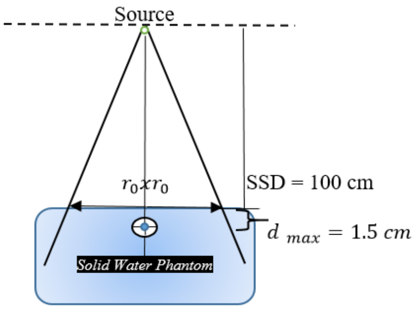

Figure 1. Schematic diagram for detector calibration setup.

Gafchromic (EBT3) film calibration

In the terms of the Gafchromic film calibration, the solid water phantom was used also and placed on the table top of linac such that the source to surface distance (SSD) was 100 cm. Seven pieces of Gafchromic films (2x7 cm^2) and one-piece with (10x10 cm^2) were used in sequence for film calibration (see Figure 2). The center of the film was located at d_{max} of the solid water phantom. The film pieces were irradiated starting from 1 Gy up to 5 Gy steps by 1 Gy of 6 MV FFF-beam (see Figure 3); finally, the irradiated films were stored for 24h in the dark box before the scan and analysis process.

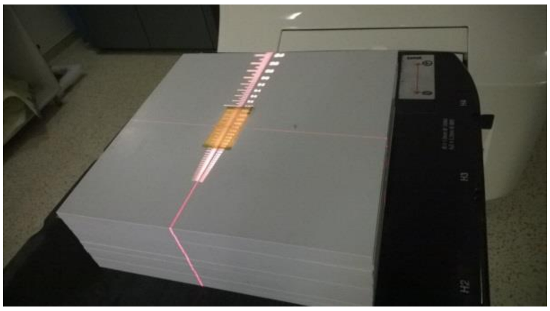

Figure 2. The film calibration setup, the Gafchromic film (EBT3) sample (2×7 cm^2) positioned on the top of solid water phantom with the source to the surface distance (SSD) 100 cm, 10 x10 cm^2 field size, and 6 MV FFF-beam.

Figure 3. Calibration series of Gafchromic films (1-5 Gy).

Total scatter factor measurement

Dosimetry

The total scatter factor, a ratio of the absorbed dose at the reference depth for a given field size, to the dose at the same depth for the reference field size, was measured at the reference depth, which for this work was 10 cm in depth. The total scatters factor can be written as:

$$S_{c,p} = \Omega^{f_{clin},f_{msr}}_{Q_{clin},Q_{msr}} = \frac{D^{f_{clin}}_{W,Q_{clin}}}{D^{f_{msr}}_{W,Q_{msr}}}. \qquad (1)$$

Where $D^{f_{clin}}_{W,Q_{clin}}$ and $D^{f_{msr}}_{W,Q_{msr}}$ are the absorbed dose to water in the clinical field f_{clin} with beam quality Q_{clin} and absorbed dose to water in the machine specific reference field f_{msr} with beam quality Q_{msr}, respectively [5, 15]. Figure 4 shows the measurement setup of the total scatter factor.

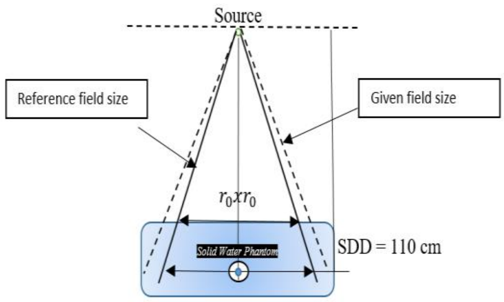

Figure 4. Schematic diagram for the total scatter factor measurement setup.

Where r_0 and *SDD* are the reference field size or let's say "machine specific reference field" and the source to detector distance, respectively. Finally, the total scatters factor was measured and recorded for Jaw-shaped beams (open beam) using calibrated detector "diamond detector" and Gafchromic (EBT3) Film**,** eight pieces of Gafchromic films were used starting from (10x10 cm^2) down to (0.5x0.5 cm^2). All measured data were evaluated and analyzed.

Results

Physical properties of the film

We found that the irradiated film had shown good stability behavior at 4 Gy. The temporal evaluation of the films revealed that the relative difference between the measured and the calculated doses decreased after the first couple of hours and increased again after a few days of irradiation using distinctive film analysis software program (ImageJ).

Figure 5 shows the relative difference (%) as a function of time (h) for ImageJ film analysis software program. The ImageJ software shows the lower fluctuation value within the 2h-72h period as well as the highest fluctuation after 72h period. The comprehensive evaluation confirmed that the optimal time interval for the scanning and analysis of the films should be within 24h to 48h after irradiation. Within this interval, the mean relative difference (%) was calculated and the relative difference was (-0.44 ± 0.14), (see Figure 5).

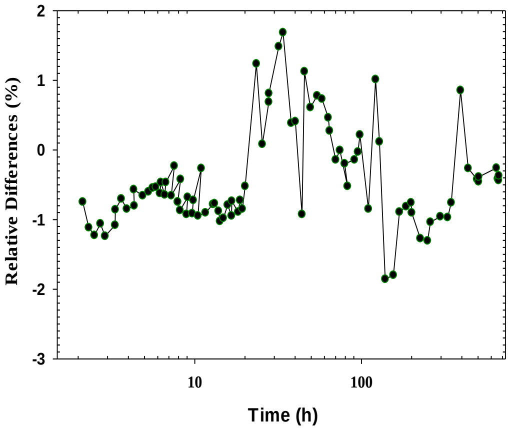

Figure 5. The mean relative differences (%) versus time (h) for ImageJ film analysis software program.

Total scatter factor measurements

Figure 6 shows the total scatter factors for the diamond detector, diode detector, and Gafchromic films as a function of field size. In the charged particle equilibrium region (CPE) when the field size is larger than 4.0 cm^2, the total scatter factors were roughly the same at the point of measurement, especially for diamond and diode detectors. On the other hand, in the charged particle dis-equilibrium region (dis-CPE) when the field size is less than 4.0 cm^2, the total scatters factor readings were lower than the actual readings near the point of measurement owing to the fluence perturbation of charged particles [16, 17]. Figure 6 shows the total scatter factors for the diamond detector, diode detector, and Gafchromic films.

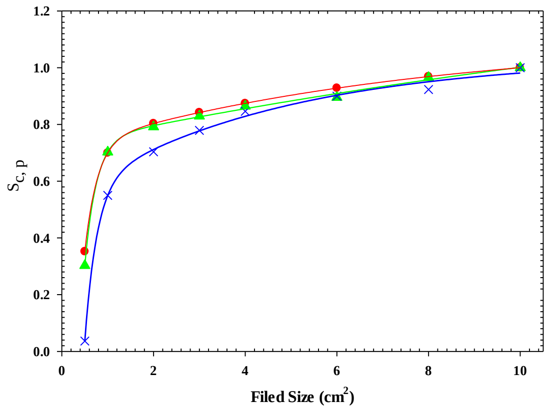

Figure 6. The total scatter factor, $S_{c,p}$, for three different dosimeters as a function of field size. Red circles: Diamond detector. Green triangles: Diode detector. Blue crosses: Gafchromic film. The lines through the measured data are the results of the best fit 'Exponential curve' to guide the eyes.

Last but not the least, the relative output factor concept is introduced to evaluate the performance of the detector with no field size, media density, or beam quality influences. The relative output factor can be written as:

$$ROF_{Diamond}^{Diode} = \frac{OF^{diode}}{OF^{diamond}} < 1, \text{ High Resolution} \qquad (2)$$

Where *ROF*, OF^{diode}, and $OF^{diamond}$ are the relative output factor, the output factor measured by diode detector, and the output factor measured by diamond detector, respectively. Figure 7 shows the relative output factors (ROF) for Diode/Diamond ($ROF_{Diamond}^{diode}$) and Film/Diamond ($ROF_{Diamond}^{film}$) combinations of 6 MV FFF photon beams with a dose rate of 800 MU/min.

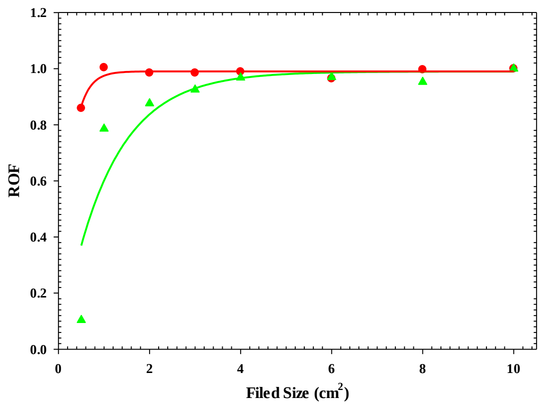

Figure 7. The Relative Output Factor (ROF) as a function of field size. Red circles: the ROF of the Diode/Diamond combination. Green triangles: the ROF of Film/Diamond combination. The lines through the measured data are the results of the best fit 'Exponential curve' to guide the eyes.

Discussion

The purpose of this study was to evaluate the performance of various dosimeters and also to determine which dosimeter is the most suitable for the total scatter factor ($S_{c,p}$) measurement at the small fields in 6 MV FFF-beam. Three different dosimeters, the ordinary ion chamber, Gafchromic (EBT3) film, and the semiconductor detectors, were used.

At a small field size, less than 1.5 cm^2, the total scatter factors readings of the diamond detector significantly differed by 14.1% and 89.6% of both diode detector and Gafchromic film readings, respectively. For the diode-diamond detectors, the total scatter factor deviation can be explained by two mechanisms 1) the detector size (volume averaging effect) and 2) the wall material of the detector. Nonetheless, the diamond detector shows more accurate total scatter factor readings at the small field size, emphases that the smaller the detector the better (more accurate) the total scatter factor readings are "i.e. high resolution". On the contrary, in the case of Gafchromic film, the total scatters factor at the same field size shows the highest deviation of both diamond and diode detectors. For the field sizes ranging between 1.5 cm^2 to 4.0 cm^2, the maximum deviation of the total scatter factors was 1.5% and 12.5% for both diode and film, respectively. In the case of large field sizes (> 4.0 cm^2), when the field is large enough to sustain equilibrium, i.e. maximum electronic range is less than the field size, in this region, one can see that the total scatter factor for various chamber types is the roughly the same with maximum deviation is around 2% and 5% between diode-diamond detectors and Gafchromic film-diamond detector, respectively. In conclusion, the film response, for small field sizes less than 4.0 cm^2, showed a worse-case scenario than other detectors, which demonstrates that the Gafchromic film is not suitable for dose measurement under the charged particle dis-equilibrium (dis-CPE) conditions and the FFF-beam. The exponential fit was used for the total scatter factor due to the fact that 1) the exponential attenuation nature of photons in the media, 2) beam hardening, the low-energy photons "scatter photons" are removed from the beam, and only primary photons remain" i.e. approaches to the pencil beam", and 3) the interaction probability, the linear attenuation coefficient, μ, has a logarithmic nature and is inversely proportional to the incident photon energy, see Figure 6.

For more justification, the relative output factor, ROF, came to use. As an alternative method to overcome the field size, beam energy, and media density effect and to evaluate the actual performance of different detectors. The $ROF^{Diode}_{Diamond}$ and $ROF^{film}_{Diamond}$ readings were within 3.5% and 4.7%, respectively, emphasizing the fact that the diode/diamond detectors show better performance and give more accurate readings than Gafchromic film under the same circumstance. On the other hand, the average deviation for both $ROF^{Diode}_{Diamond}$ and $ROF^{film}_{Diamond}$ readings was within 0.9% and 13.7% at the large field sizes, larger than 4.0 cm^2, see Figure 7. For ultra-small field size (0.5x0.5 cm^2), the ROF for the previous combinations significantly differed with the maximum deviations of 14.1% and 89.6%, respectively. Similarly, the ROF was also fitted by exponential fitting due to the exponential attenuation nature of photons in the media, beam hardening, besides the logarithmic nature of the linear attenuation coefficient, μ.

Several studies have been associated with small field dosimetry [5, 8, 9, 11, 12, 15, 18-24], using different detectors under charged particle dis-equilibrium conditions and the flatting filter beam (FFB) to provide the same conclusion; the smaller the detector the better (more accurate) the total scatter factor readings are. In this study, the same behavior has been recognized for various detectors under the charged particle dis-equilibrium and FFF-beam, the smaller the detector the more accurate total scatter factor readings are, demonstrating that the detector behavior is flatting filter-independent.

The limitation of this study was the use of solid water phantom without any consideration for the media density effect. For more accurate results, it is recommended to evaluate the total scatter factor for different density media. Moreover, the current study was only carried out on the one linear accelerator (Varian True beam). Therefore, the evaluations on various linacs would be useful for more comprehensive results.

Conclusion

We presented a comprehensive study to evaluate the diamond detector, diode detector, and Gafchromic films performance under charged particle dis-equilibrium conditions and FFF-beam. We demonstrated that the diamond detector was the more accurate detector, especially for ultra-small field size (0.5x0.5 cm^2). For the large field sizes, larger than 4.0 cm^2, the deviation of the total scatter factors among three different detectors was less than 5%. In addition, we presented the relative output factor (ROF) as the total scatter factor measured by a specific dosimeter (x) to that measured by a diamond detector ($OF_x/OF_{diamond}$). The relative output factor readings for the small field size (< 1.5 cm^2) of 6 MV FFF-beam using the combination of the diode/diamond detector were the most appropriate combination with a 14.1% deviation. In contrast, the Gafchromic film/diamond combination was less precise for the FFF-beam measurement, especially for the ultra-small field. In conclusion, any further investigation is highly recommended to be accomplished by the diamond detector.

References

1. Masanga W, Tangboonduangjit P, Khamfongkhruea C, Tannanonta C. Determination of small field output factors in 6 and 10 MV flattening filter free photon beams using various detectors. InJournal of Physics: Conference Series 2016 Mar 1 ; 694(1): 012027.
2. Sharma SD. Unflattened photon beams from the standard flattening filter free accelerators for radiotherapy: Advantages, limitations and

challenges. Journal of Medical Physics/Association of Medical Physicists of India. 2011 Jul;36(3):123.
3. Kragl G, af Wetterstedt S, Knäusl B, Lind M, McCavana P, Knöös T, et al. Dosimetric characteristics of 6 and 10 MV unflattened photon beams. Radiotherapy and Oncology. 2009 Oct 1;93(1):141-6.
4. Hrbacek J, Lang S, Klöck S. Commissioning of photon beams of a flattening filter-free linear accelerator and the accuracy of beam modeling using an anisotropic analytical algorithm. International Journal of Radiation Oncology* Biology* Physics. 2011 Jul 15;80(4):1228-37.
5. Huq MS, Hwang MS, Teo TP, Jang SY, Heron DE, Lalonde RJ. A dosimetric evaluation of the IAEA-AAPM TRS 483 code of practice for dosimetry of small static fields used in conventional linac beams and comparison with IAEA TRS-398, AAPM TG 51, and TG 51 Addendum protocols. Medical physics. 2018 Sep;45(9):4257-73.
6. Dai X, Zhao Y, Liang Z, Dassarath M, Wang L, Jin L, et al. Volumetric-modulated arc therapy for oropharyngeal carcinoma: a dosimetric and delivery efficiency comparison with static-field IMRT. Physica Medica. 2015 Feb 1;31(1):54-9.
7. Georg D, Knöös T, McClean B. Current status and future perspective of flattening filter free photon beams. Medical physics. 2011 Mar;38(3):1280-93.
8. Das IJ, Ding GX, Ahnesjö A. Small fields: nonequilibrium radiation dosimetry. Medical physics. 2008 Jan;35(1):206-15.
9. Charles PH, Cranmer-Sargison G, Thwaites DI, Crowe SB, Kairn T, Knight RT, et al. A practical and theoretical definition of very small field size for radiotherapy output factor measurements. Medical physics. 2014 Apr;41(4):041707.
10. Al Atawneh S. Analytical Formula for the total scatter factor of the Small Radiation Field Size. 2021; 7(3): 152-60.
11. Al Atawneh SJ. Empirical Formalism for the Phantom Scatter Factor of Small Fields: Using Different Density Media. International Journal of Medical Physics, Clinical Engineering and Radiation Oncology. 2021 Dec 24;11(1):36-47.
12. Parwaie W, Refahi S, Ardekani MA, Farhood B. Different dosimeters/detectors used in small-field dosimetry: Pros and cons. Journal of medical signals and sensors. 2018 Jul;8(3):195-203.
13. Lechner W, Palmans H, Sölkner L, Grochowska P, Georg D. Detector comparison for small field output factor measurements in flattening filter free photon beams. Radiotherapy and oncology. 2013 Dec 1;109(3):356-60.
14. Dwivedi S, Kansal S, Dangwal VK, Bharati A, Shukla J. Dosimetry of a 6 MV flattening filter-free small photon beam using various detectors. Biomedical Physics & Engineering Express. 2021 May 11;7(4):045004.
15. Zhu TC, Ahnesjö A, Lam KL, Li XA, Ma CM, Palta JR, et al. Report of AAPM Therapy Physics Committee Task Group 74: in-air output ratio, for megavoltage photon beams. Medical physics. 2009 Nov;36(11):5261-91.
16. Nahum AE. Perturbation effects in dosimetry: Part I. Kilovoltage x-rays and electrons. Physics in Medicine & Biology. 1996 Sep 1;41(9):1531.
17. Laub WU, Wong T. The volume effect of detectors in the dosimetry of small fields used in IMRT. Medical physics. 2003 Mar;30(3):341-7.
18. Ding GX, Duggan DM, Coffey CW. Commissioning stereotactic radiosurgery beams using both experimental and theoretical methods. Physics in Medicine & Biology. 2006 May 4;51(10):2549.
19. Sauer OA, Wilbert J. Measurement of output factors for small photon beams. Medical physics. 2007 Jun;34(6Part1):1983-8.
20. Klein DM, Tailor RC, Archambault L, Wang L, Therriault-Proulx F, Beddar AS. Measuring output factors of small fields formed by collimator jaws and multileaf collimator using plastic scintillation detectors. Medical physics. 2010 Oct;37(10):5541-9.
21. Bassinet C, Huet C, Derreumaux S, Brunet G, Chéa M, Baumann M, et al. Small fields output factors measurements and correction factors determination for several detectors for a CyberKnife® and linear accelerators equipped with microMLC and circular cones. Medical physics. 2013 Jul;40(7):071725.
22. Nasir MK, Amjad N, Razzaq A, Siddique T. Measurement and analysis of PDDs profile and output factors for small field sizes by CC13 and micro-chamber CC01. International Journal of Medical Physics, Clinical Engineering and Radiation Oncology. 2017;6(01):36.
23. Islam MR, Watabe H, Stefano A. Measurement and Comparison of Output Factors Using Two Detectors for NOVAC7 IntraOperative Radiotherapy Accelerator. International Journal of Medical Physics, Clinical Engineering and Radiation Oncology. 2020 Mar 25;9(2):52-61.
24. Dufreneix S, Di Bartolo C, Bremaud M, Mesgouez J, Legrand C, Autret D. P10. How to choose a detector for small fields measurements?. Physica Medica: European Journal of Medical Physics. 2016 Dec 1;32:371.